International Journal of Greenhouse Gas Control 83 (2019) 128–139

Contents lists available at ScienceDirect

International Journal of Greenhouse Gas Control

journal homepage: www.elsevier.com/locate/ijggc

Geologic CO_2 sequestration and permeability uncertainty in a highly heterogeneous reservoir

Richard S. Jayne*, Hao Wu, Ryan M. Pollyea

Department of Geosciences, Virginia Polytechnic Institute & State University, Blacksburg, VA, United States

ARTICLE INFO

Keywords:
Numerical modeling
Permeability
Heterogeneity
CO_2 sequestration
Columbia River Basalt Group

ABSTRACT

To understand the implications of permeability uncertainty in basalt-hosted CCS reservoirs, this study investigates the feasibility of industrial-scale CCS operations within the Columbia River Basalt Group (CRBG). It is generally accepted that plausible constraints on *in situ* fracture-controlled permeability distributions are unknowable at reservoir scale. In order to quantify the effects of this permeability uncertainty, stochastically generated and spatially correlated permeability distributions are used to create 50 synthetic reservoir domains to simulate constant pressure CO_2 injections. Results from this research illustrate that permeability uncertainty at the reservoir-scale significantly impacts both the accumulation and distribution of CO_2. After 20 years of injection the total volume of CO_2 injected in each simulation ranges from 2.4 MMT to 40.0 MMT. Interestingly, e-type calculations show that the mean CO_2 saturation over the ensemble of 50 simulations is concentric around the injection well, however, ensemble variance shows an ellipse of uncertainty that trends parallel to the long axis of CRBG permeability correlation (N40°E). These results indicate that *a priori* knowledge of permeability correlation structure is an important operational parameter for the design of monitoring, measuring, and verification strategies in highly heterogeneous CCS reservoirs.

1. Introduction

Spatial heterogeneities are present at all geologic scales, from pore (Chang et al., 2016) to reservoir scales (Doughty and Pruess, 2004). Understanding how spatial heterogeneity affects fluid flow is critical for engineered carbon capture and storage (CCS) reservoirs in terms of monitoring, management, and verification (MMV). Reservoirs that are targeted for CCS require extensive site characterization to ensure that the reservoir meets the requirements for capacity, injectivity, and confinement for a given CCS project. Numerical models are commonly used to predict what effects a large-scale CO_2 injection will have on the target reservoir and the behavior of the CO_2 plume. However, many numerical modeling studies employ a homogeneous representation of the geologic media (Van der Meer, 1995; Pruess and Garcia, 2002; Pruess et al., 2003). For example, at the reservoir-scale it is common to implement a layered heterogeneity approach with internally homogeneous rock properties. Doughty (2010) simulates an injection of 1.1 million metric tons of CO_2 into a dipping sedimentary basin to investigate the spatial and temporal evolution of the CO_2 plume. While this approach may be reasonable for some geologic environments, it is also well established that uncertainty with the model parameters, such as, permeability will strongly affect the direction and extent of the CO_2 plume (Doughty, 2010). Moreover, Doughty and Pruess (2004) investigate the physical processes associated with the sequestration of supercritical CO_2 and show that the highly heterogeneous nature of geologic media results in the formation of preferential flow paths which have a significant impact on the overall behavior of the injected CO_2.

Reservoir integrity within highly heterogeneous reservoirs is one of the main concerns surrounding the idea of industrial-scale CCS projects because leakage from CO_2 storage sites may have negative health, safety, and environmental (HSE) impacts at the surface. The difficulty in reducing HSE risks, is locating the source of the CO_2 leak from the reservoir or any wells within the target formation. Previous works have investigated issues of CO_2 leakage from a CO_2 storage site into surface waters (Oldenburg and Lewicki, 2006), CO_2 leakage through fault or fracture pathways (Neufeld et al., 2009), and leakage through plugged and abandoned wells (Pawar et al., 2009). The ability to monitor a CO_2 plume post-injection and subsequent leaks is the first step in mitigating these potential HSE risks. However, some monitoring efforts require *a priori* knowledge of the location of the CO_2 plume (i.e., well-based monitoring). This requires site-specific predictions from detailed characterization of the subsurface, which is a complicated and complex endeavor (Price and Oldenburg, 2009). Quantifying, understanding, and minimizing these risks effectively is a necessity if industrial-scale

* Corresponding author.
E-mail address: rjayne@vt.edu (R.S. Jayne).

https://doi.org/10.1016/j.ijggc.2019.02.001
Received 23 May 2018; Received in revised form 19 October 2018; Accepted 2 February 2019

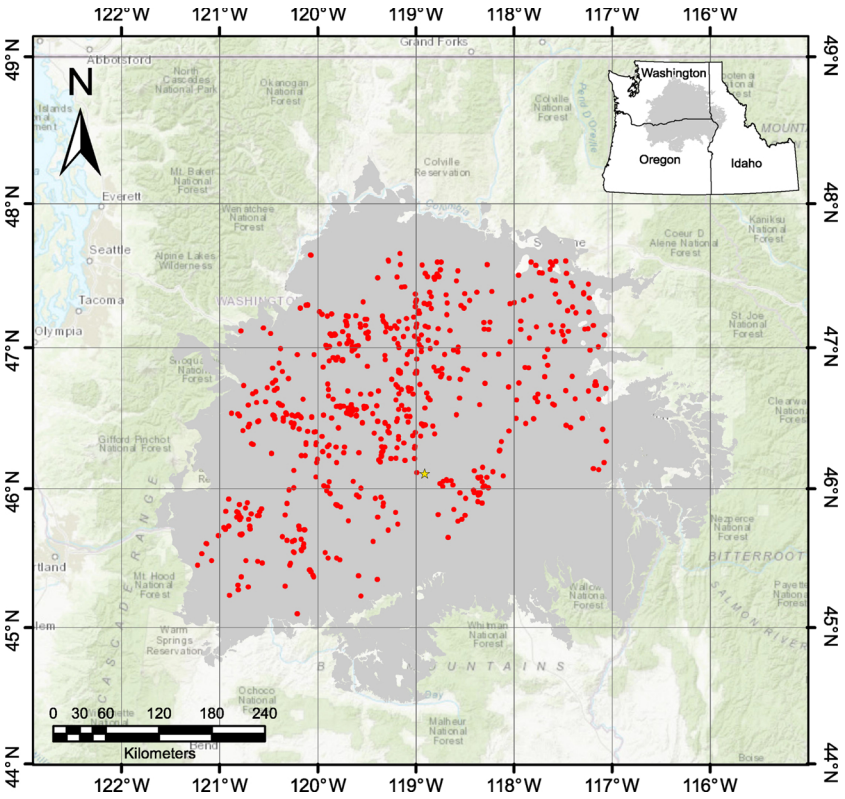

Fig. 1. Map showing the areal extent of the Columbia River Basalts shaded in grey. Wells with permeability data compiled by Jayne and Pollyea (2018) within the CRBG are shown in red and the Wallula Pilot Borehole is denoted by the yellow star. (For interpretation of the references to color in this figure legend, the reader is referred to the web version of this article.)

CO_2 injections are to become a viable option to mitigate climate change (Navarre-Sitchler et al., 2013).

A number of geologic formations have been investigated over the years to study their potential for CCS. Sedimentary formations have been extensively studied due to their ubiquity, large storage capacity, and relatively high permeabilities, which are all required for large-scale CO_2 injections (Bachu, 2003; Metz et al., 2005). Other options for CCS include depleted oil/gas reservoirs and deep, un-mineable coal seams (Brennan and Burruss, 2003). In addition, flood basalt formations have been gaining recognition as suitable reservoirs for industrial-scale CCS. Unlike sedimentary aquifers that keep the CO_2 trapped via capillary and solubility trapping mechanisms (Wu et al., 2018), igneous rocks have a higher potential for permanent geomechanical trapping of CO_2 (McGrail et al., 2006; Matter et al., 2007; Matter and Kelemen, 2009; Zakharova et al., 2012; Pollyea and Rimstidt, 2017). Geochemical trapping involves a series of chemical reactions between the CO_2, aquifer water, and reservoir rock resulting in the precipitation of thermodynamically stable and environmentally benign carbonate minerals. Recent developments at the CarbFix CCS pilot in Iceland (Matter et al., 2016) and the Wallula Basalt Pilot Project located in eastern Washington (McGrail et al., 2017) have shown that basalt reservoirs are highly effective for permanent mineral trapping on the basis of CO_2-water-rock interactions. Specifically, pilot-scale basalt CCS at the CarbFix project showed 95% permanent CO_2 mineralization within two years of injection (Matter et al., 2016). However, despite the effectiveness of trapping CO_2 via mineralization, the volumes injected in both pilot projects (270 tons CO_2 at CarbFix, 1000 tons CO_2 at Wallula) are far from the scales required to mitigate climate change. Upscaling from a pilot project to an industrial-scale CO_2 injection requires a detailed characterization of the subsurface, which introduces a significant amount of uncertainty associated with reservoir parameters which affect the injectivity, capacity, and confinement of the target reservoir (Chadwick et al., 2008).

Chadwick et al. (2008) outlines the importance of reservoir characterization and how it is a necessary step to characterize both the hydrologic and structural properties of the target reservoir for a CCS project. For flood basalt reservoirs this can be challenging because it is generally accepted that plausible constraints on *in situ* permeability distributions are unknowable at reservoir scale. Previous studies have investigated this issue, for example, Pollyea et al. (2014) quantifies the effects of fracture-controlled heterogeneity by using stochastically generated model domains along with Monte Carlo CO_2 injection modeling to show the highly variable sealing behavior within the low-volume Snake River Plains basalts. Additionally, there remains significant uncertainty with respect to multiphase flow within heterogeneous media at all scales. For example, the effects of pore-scale heterogeneity on supercritical CO_2-water flow and relative permeability saturation curves have been investigated by Chang et al. (2016). Gierzynski and Pollyea (2017) investigate outcrop-scale CO_2 flow within a basalt fracture network and show that CO_2 tends to accumulate at fracture intersection, which may yield self-sealing reservoir characteristics as mineralization focuses at the union of branching fractures. Bosshart et al. (2018) demonstrates how heterogeneities and a range of petrophysical properties can significantly affect the CO_2 injection rate and storage capacity by modeling CO_2 injections into different depositional environments. Moreover, uncertainty in permeability distributions at any scale, especially site-scale or larger can have a substantial impact on the efficacy of hydrogeologic models, as well as, numerical model-based risk assessment (NETL, 2011; Pollyea and Fairley, 2012; Pollyea et al., 2014). To account for this uncertainty, stochastic methods have been increasingly deployed to understand how spatial permeability uncertainty affects feasibility assessments in fractured basalt reservoirs (Srivastava, 1994a; Li et al., 2005; Pollyea and Fairley, 2012; Pollyea et al., 2014; Popova et al., 2014; Gierzynski and Pollyea, 2017). These methods constrain spatial permeability distributions on the basis of a known (or assumed) probability distributions and spatial correlation models (e.g., semivariogram). By utilizing spatial correlation models and stochastic methods, this study is designed to assess the uncertainty of fracture-controlled permeability at the reservoir scale associated with a CO_2 injection scenario. As a result, this study provides a link between permeability heterogeneity and CO_2 storage efficiency, as well as providing a first-order approximation of the level of sensitivity

associated with CO_2 storage in highly heterogeneous hydrogeological systems.

1.1. Geologic setting

1.1.1. Columbia River Basalt Group

The Columbia River Basalt Group (CRBG) is a continental large igneous province in the northwest United States (Fig. 1), and comprises a layered assemblage of ~300 Miocene-age flood basalts with an areal extent of 200,000 km^2, aggregate thickness of 1–5 km, and total estimated volume of 224,000 km^3 (Reidel et al., 2002; McGrail et al., 2009). The CRBG has been extensively studied due to its wide range of resource potential, including (1) groundwater production (Burns et al., 2011; Kahle et al., 2011), (2) nuclear waste storage (e.g., Gephart et al. (1983), (3) natural gas storage (Reidel et al., 2002), (4) geologic CO_2 sequestration (McGrail et al., 2017), and (5) geothermal resources (Burns et al., 2016). Among the principal challenges in assessing the feasibility of engineered CRBG reservoirs is to understand how fracture-controlled reservoir properties (i.e., permeability and porosity) affect both local- and regional-scale fluid flow. These fracture-controlled reservoir properties are governed by individual basalt flow morphology, which is characterized by: (1) densely fractured, vesicular flow-tops, (2) a central entablature comprising narrow, fanning columnar joints, and (3) lower colonnades with vertical, column bounding joints (Fig. 2) (Mangan et al., 1986). Within CRBG flows, *in situ* pumping tests reveal that permeability ranges over thirteen orders of magnitude with the entablature zone generally inhibiting groundwater flow, while densely fractured flow tops and flow bottoms are highly productive (Kahle et al., 2011; Jayne and Pollyea, 2018) (Fig. 3A). To further complicate CRBG reservoir characterization, individual basalt flows exhibit km-scale lateral dimensions and vertical dimensions from cm-scale to greater than 70 m (Mangan et al., 1986).

1.1.2. Wallula Pilot Borehole

As part of the Big Sky Carbon Sequestration Partnership (BSCSP), the U.S. Department of Energy identified the Columbia River Basalt Group (CRBG) as a primary target formation for CCS development in the Pacific Northwest. The CRBG was chosen on the basis of its relatively high CO_2 storage estimates (10–50 Gt CO_2), potential for CO_2 isolation, and generally favorable reservoir characteristics (Litynski et al., 2006; McGrail et al., 2006, 2017; Rodosta et al., 2011). In order to locate a suitable site for a pilot injection, seismic surveys were conducted in Walla Walla County, WA, which identified areas where

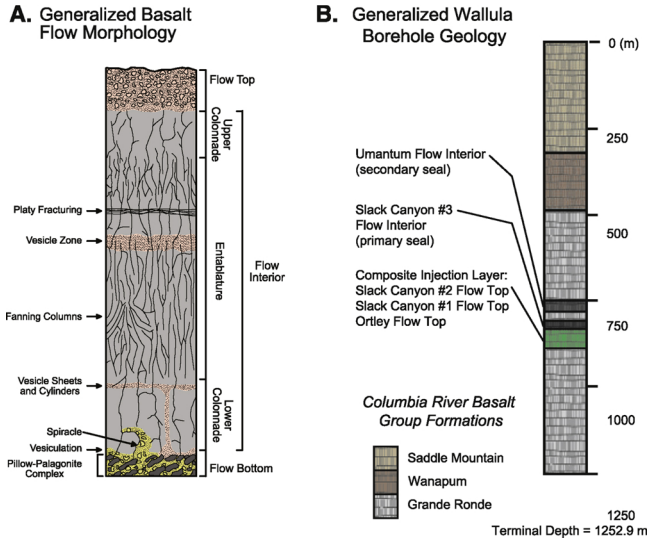

Fig. 2. A. Individual CRBG flow morphology (modified from Reidel et al. (2002)). B. Generalized geology within the Wallula Pilot Borehole.

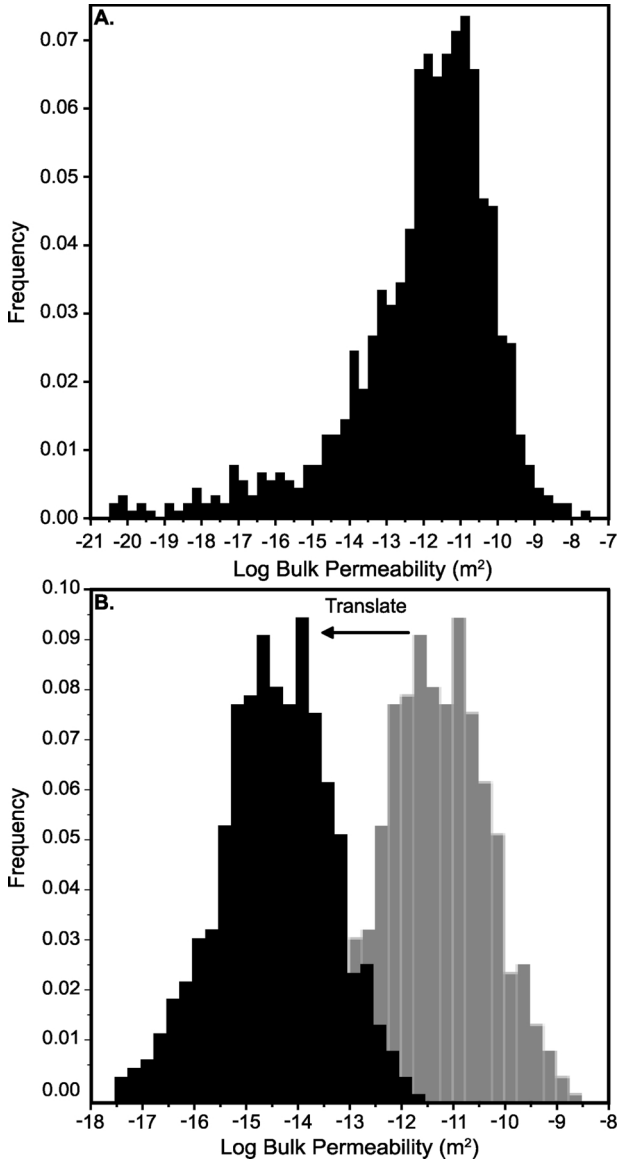

Fig. 3. A. Histogram of log permeability from well data compiled by Jayne and Pollyea (2018). B. Histogram of the filtered permeability data to represent the high permeability flow tops. The mean of log permeability is $-11.5\ m^2$ (grey), in order to make this range of permeabilities more representative at the depth of the injection zone the permeability distribution is translated downward so that the mean log permeability is $-14.5\ m^2$, which is congruent with field test from the Wallula borehole.

major geologic structures would not preclude a CO_2 injection (McGrail et al., 2011). In January 2009 drilling of the Wallula Pilot Borehole began and was completed in April 2009. The Wallula Pilot Borehole reaches a total depth of 1,253 m and intersects three CRBG formations: Saddle Mountain, Wanapum, and Grande Ronde (McGrail et al., 2009). The target formation for injection is the Grande Ronde Basalt, of which the Wallula Pilot Borehole intersects 26 flows and 7 members. A candidate (composite) injection zone was identified at 828–887 m depth, spanning three brecciated interflow zones within the Grande Ronde Formation (McGrail et al., 2009). Hydrologic characterization of these three zones show that they represent a single hydraulic unit with relatively high permeability and are bounded by thick low permeability flow interiors, which act as a natural caprock (McGrail et al., 2009). In 2013, a nominal 1000 metric tons (MT) of supercritical CO_2 was injected at the Wallula Pilot Borehole over the course of three weeks. Since the injection, results have been published validating the reactivity

of supercritical CO_2 with basalts at the Wallula Pilot Borehole (McGrail et al., 2017). Though these results are promising, transitioning to an industrial-scale CO_2 injection comes with a significant amount of uncertainty, and before an industrial-scale injection can be implemented a better understanding of these uncertainties is required. This study is designed to bound the uncertainty associated with incomplete knowledge of CRBG permeability during industrial-scale CO_2 injections. Specifically, we implement stochastic simulation strategy in combination with known geologic information from the Wallula borehole to quantify how permeability variability affects CO_2 storage capacity and leakage potential within a synthetic CCS reservoir comprising CRBG basalt.

2. Methods

This study combines geostatistical reservoir simulation with multiphase, multicomponent numerical modeling to investigate the influence that the spatial distribution of permeability has on the accumulation and distribution of the injected supercritical CO_2 within the Grande Ronde formation of the CRBG. The model scenario is designed to represent a large-scale constant pressure injection of supercritical CO_2 into the composite injection zone (775–875 m) at the Wallula Pilot Borehole. While the hydrologic characterization within the Wallula Pilot Borehole has been extensive, the permeability distribution at intermediate- to long-range spatial scales is poorly constrained. As a result, this study uses a geostatistical analysis to constrain permeability at the reservoir-scale and provide a first-order approximation of the uncertainty associated with a large-scale CO_2 injection into a fracture-dominated, highly heterogeneous basalt reservoir.

2.1. Model domain

The model domain for this study comprises an areal extent of 5,000 m × 5,000 m × 1,250 m, which represents ground surface to 1,250 m depth with the Wallula Pilot Borehole centrally located (Fig. 4). This domain is discretized into 530,000 grid blocks with dimensions of 50 m × 50 m × 25 m. For this model, the CRBG is conceptualized on the basis of basalt flow morphology, which is a layered heterogeneous system consisting of highly fractured flow tops (high permeability) and flow interiors (low permeability). However, this layered heterogeneity does not take into account the wide range of permeability within individual basalt flow units, which are known to be internally heterogeneous due to the ubiquitous fracture networks within CRBG basalt. In order to account for the wide range of fracture-controlled permeability within the composite injection zone (775–875 m depth), sequential indicator simulation (sisim) is employed to generate stochastic permeability distributions for the injection zone (Deutsch and Journel, 1998). In this approach, the sisim routine selects grid cells in random order and solves the ordinary kriging equations on the basis of (1) the cumulative distribution function for CRBG permeability, (2) known data points, which are the borehole permeability tests from the Wallula borehole, (3) grid cells previously simulated by the sisim routine, and (4) the chosen spatial correlation model, which for this study is an anisotropic semivariogram model developed by Jayne and Pollyea (2018).

Jayne and Pollyea (2018) show that permeability within the Columbia River Plateau exhibits a direction of maximum and minimum spatial correlation oriented at N40°E and N130°E, respectively. In order to calculate these spatial correlation models Jayne and Pollyea (2018) compiled a regional database of CRBG permeability values from wells within the CRBG (Fig. 1) to calculate semivariograms. To do this, permeability values were filtered on two standard deviations of the mean to ensure only the highly productive flow tops and bottoms were included in the calculations (Fig. 3B). The present study adopts this convention to constrain the ranges of permeability within the high permeability zones that are representative of the composite injection zone. This results in a range of log permeability from $-8.5\,m^2$ to $-14.5\,m^2$ with a median log permeability value of $-11.5\,m^2$. However, the present study is focused on permeability at depths greater than 750 m, where the log permeability in the Wallula Pilot Borehole is $\sim -14.5\,m^2$. In order to account for this, the permeability distribution is translated so that the variability of permeability is maintained but the mean permeability is representative of the composite injection in the Wallula Pilot Borehole. This results in a new range of log permeability from $-11\,m^2$ to $-17\,m^2$. Using this approach, a total of 50 equally probable injection zones are simulated and inserted into the model domain between 775 and 875 m. It is important to note that sisim typically honors the original probability distributions of the original

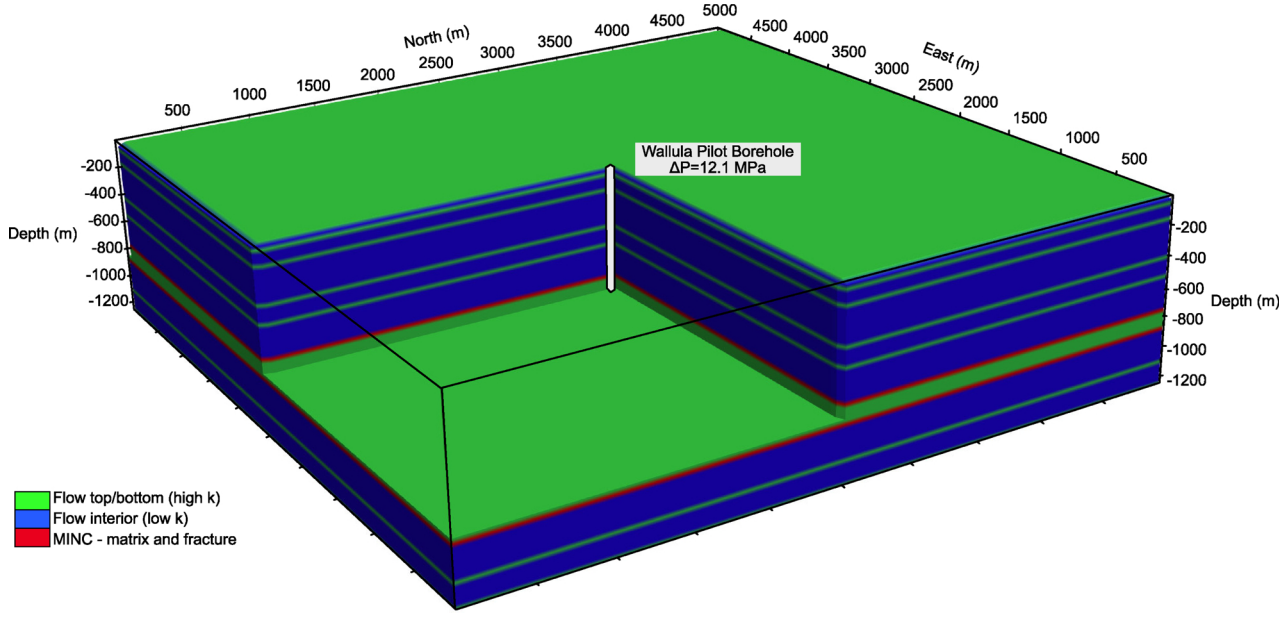

Fig. 4. Model domain for CO_2 injection modeling study. The composite injection zone is bounded by the two red layers, the latter of which are specified as multiple interacting continua (MINC) to represent fracture-matrix flow within the bounding entablature units. (For interpretation of the references to color in this figure legend, the reader is referred to the web version of this article.)

dataset with minor ergotic fluctuation. In this study, the resulting 50 equally-probable, spatially correlated permeability distributions vary slightly about the mean, with an average log permeability of $-14.34\,m^2$ and a standard deviation of 0.27. While there is some variability in permeability distribution between the 50 synthetic reservoirs, each reproduces an equally-probable permeability distribution for the given dataset shown in Fig. 3B. In order to model the effects of fracture-matrix flow within the entablature zones bounding the composite injection layer, the multiple-interacting-continua (MINC) method is utilized to produce a dual-permeability model that is representative of columnar jointing typical of basalt flow entablatures. The MINC method is a generalized dual-porosity concept, which allows for partitioning of the flow domain into different computational volumes within each element (Pruess, 1992). In this approach, grid blocks are "nested" within one another allowing a single grid block to be defined by multiple finite elements (multiple rock properties can be used, such as, for fractured and unfractured rock matrix). A total of 50-equally probable synthetic reservoirs are simulated in which permeability within the injection zone is stochastically generated by sequential simulation and the entablature zones bounding the injection layer are modeled as a dual-continuum to represent columnar jointing.

For this modeling study, the relative permeability and capillary pressure models along with the bulk fluid and rock properties are listed in Table 1. The bulk reservoir properties for the CRBG are consistent with those of Gierzynski and Pollyea (2017) and Zakharova et al. (2012). Relative permeability and capillary pressure curves are used to simulate the effects of multiphase flow in a CO_2 and water system. Parameters for relative permeability and capillary pressure are described by the van Genuchten model, the van Genuchten parameters in Table 1 are based off of Pollyea (2016) where the influence of relative permeability on injection pressure is investigated within a mafic reservoir. Pollyea (2016) shows that for a constant mass CO_2 injection, maximum injection pressure can vary from 5–60 MPa over a range of van Genuchten parameters. Based off of these results, the phase interference (λ) and residual liquid saturation (S_{lr}) parameters corresponding to a maximum injection pressure of 25 MPa are chosen to keep CO_2 accumulation and distribution estimates modest for a constant pressure CO_2 injection.

2.2. Numerical CO_2 flow simulation

In order to investigate how the spatial distribution of permeability affects CCS reservoir performance in a flood basalt reservoir, CO_2 injection is simulated within each equally probable synthetic reservoir at constant pressure for 20 years. Constant pressure injections are simulated for this study within the composite injection zone at the Wallula Pilot Borehole to not only investigate the distribution of supercritical CO_2, but also compare the total mass of CO_2 injected over all 50 simulations. A constant overpressure of 12.1 MPa is used to simulate the CO_2 injection. This injection pressure represents 95% of the borehole breakout pressure as calculated by Pollyea (2016), borehole breakout pressure is used so that the maximum amount of CO_2 can be injected in each simulation without borehole failure. The code selection for this study is TOUGH3 (Jung et al., 2017) compiled with the ECO2M module (Pruess, 2011). TOUGH3 solves energy and mass conservation equations for nonisothermal, multiphase flows in a porous geologic media. The ECO2M module simulates mixtures of H_2O–NaCl–CO_2, within the following ranges for temperature, pressure, and salinity conditions: 10 °C ≤ Temperature ≤ 110°C, pressures ≤60 MPa, and salinity from zero up to full halite saturation. ECO2M can also simulate all possible phase conditions for CO_2 – brine mixtures, including transitions between super- and sub-critical CO_2 as well as phase transitions between liquid and vapor CO_2 (Pruess, 2011).

Table 1
Model parameters.

	Matrix	Fracture	Flow top	Basal boundary
Density ($kg{\cdot}m^{-3}$)	2900.0	2300.0	2300.0	2900.0
Porosity	0.05	0.1	0.3	0.05
Permeability(m^2)	10^{-20}	10^{-16}	varies	10^{-20}
Thermal Conductivity ($W{\cdot}m{\cdot}°C^{-1}$)	2.11	2.11	2.11	2.11
Heat Capacity ($J{\cdot}kg^{-1}{\cdot}°C^{-1}$)	840	840	840	840

van Genuchten parameters

Relative Permeability		Capillary Pressure	
λ	0.550	λ	0.457
S_{lr}	0.30	S_{lr}	0.0
S_{ls}	1.0	α (Pa^{-1})	5.e−5
S_{gr}	0.25	P_{max} (Pa)	1e.7
		S_{ls}	0.999

Initial conditions are specified with a hydrostatic pressure gradient ranging from 0.101 MPa (1 atm at ground surface) to 12.3 MPa at the bottom of the Wallula Pilot Borehole. Initial temperature is calculated by using the regional heat flux ~65 mW/m^2 (Pollack et al., 1993) as a thermal boundary at the base of the model and a constant temperature of 10 °C at ground surface, resulting in a linear temperature gradient from 10 °C at the surface to 50 °C, and thermal effects are accounted for in the simulations. These initial conditions are consistent with the field measurements taken at the Wallula Pilot Borehole (McGrail et al., 2009). Within the composite injection zone, initial temperature and pressure conditions range from 35–38 °C and 7.7–8.4 MPa, which are within the supercritical field for CO_2. Dirichlet boundary conditions are specified at the upper boundary of the model domain to hold pressure and temperature constant at ground surface and at the lateral boundaries of the model domain to maintain temperature and pressure gradients in the far-field.

As with all modeling studies, a brief mention of the limitations of this model is warranted. This modeling study does not account for basalt dissolution or secondary mineral precipitation, and, as a result, this modeling study represents a conservative estimate of CO_2 storage capacity and leakage potential. Consequently, permeability alteration due to secondary mineral precipitation is neglected; however, we note that empirical permeability–porosity relationships have not yet been quantified in basalt reservoirs. Additionally, relative permeability hysteresis is not accounted for in the simulations, because only the injection phase of a CCS project is simulated so there is no imbibition for the wetting phase. Similarly, chemical diffusion is not accounted for because CO_2 is being continuously injected throughout the entire simulation resulting in a high Péclet number, which means the transport of mass and heat is dominated by advection.

2.3. Data analysis

The ensemble of 50 simulations are analyzed using e-type estimates on a grid cell by grid cell basis to quantify the average overall behavior of CO_2 at the reservoir scale, as well as, the corresponding spatial uncertainty (Deutsch and Journel, 1998). In this approach, the mean ($N = 50$) CO_2 saturation ($\bar{S}_{(x,y,z)}$) within each grid cell is computed as:

$$\bar{S}_{(x,y,z)} = \frac{1}{50}\sum_{i=1}^{50} S_{i(x,y,z)} \tag{1}$$

where $S_{i(x,y,z)}$ is the modeled CO_2 saturation for simulation i at location (x, y, z). Similarly, the variance ($s^2_{x,y,z}$) associated with Eq. (1) for each grid cell is computed as:

$$s^2_{(x,y,z)} = \frac{1}{50}\sum_{i=1}^{50} (S_{i(x,y,z)} - \bar{S}^2_{i(x,y,z)}) \tag{2}$$

In the present study, the mean and variance are calculated for free-phase CO_2 saturation over all 50 simulations to investigate the uncertainty associated with a CO_2 injection into the Columbia River Basalt group.

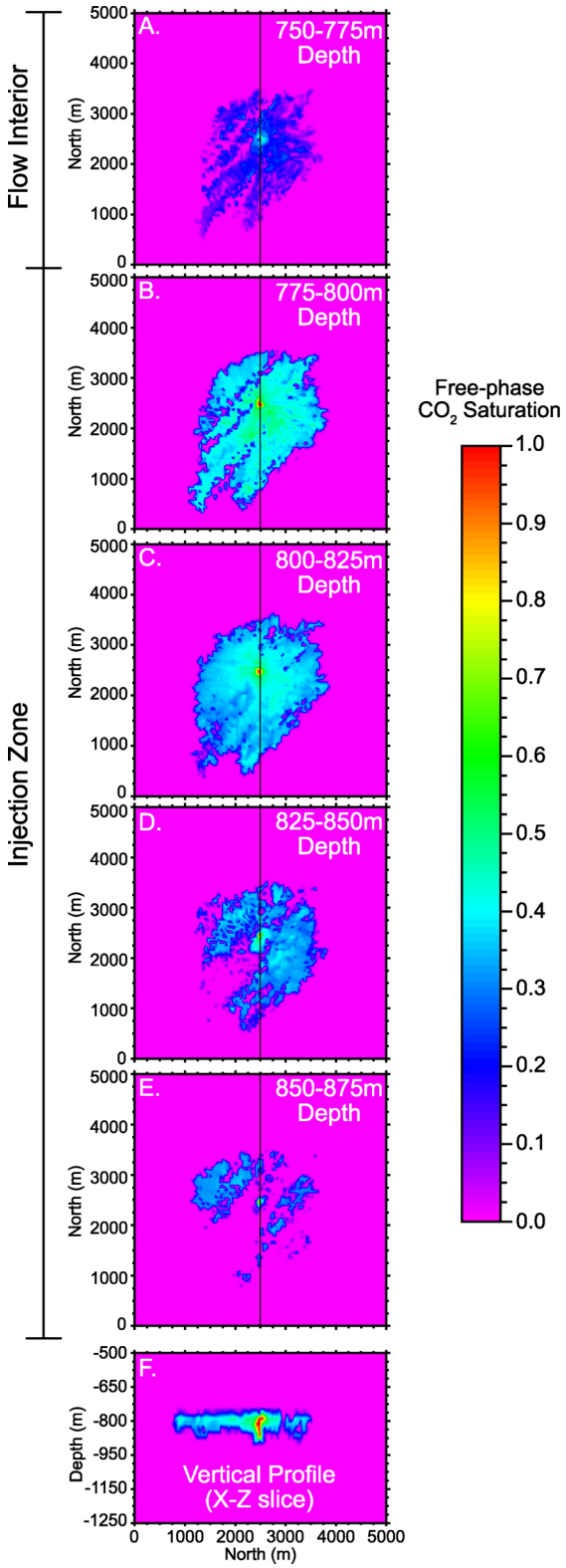

Fig. 5. Single realization (20) of a 20-year constant pressure CO_2 injection. A. Represents the layer above the injection zone and illustrates that free-phase CO_2 is present within the fractures. B–E. Each represents an individual injection layer within the Wallula Pilot Borehole. F. A vertical north-south profile through the center (indicated by the black lines in A–E) of the model domain.

3. Results and discussion

Each numerical model accounts for 20 years of simulation time, in which supercritical CO_2 is injected within the Wallula Pilot Borehole at a constant pressure. For each analysis the simulations are referred to by an integer index (1–50). In order to maintain consistency and facilitate comparison each analysis includes simulation 20 because the total mass of CO_2 injected for this simulation is close to the ensemble mean. Simulation 20 also illustrates the effect of spatially correlated permeability within the CRBG, which is represented by Fig. 5 and shows free-phase CO_2 saturation within each layer of the injection zone after 20 years. When comparing the accumulation and distribution of CO_2 within each layer in Fig. 5, it is clear that top injection layer (Fig. 5B) has the largest volume of CO_2 and this is due to buoyancy forces and the high permeability pathways that have formed due to the spatial heterogeneity. The combination of buoyancy-driven upward CO_2 flow and permeability heterogeneity results in CO_2 saturation patterns from the injection zone superimposed on the overlying entablature zone, which is the reservoir confining layer (Fig. 5A). As a result, permeability heterogeneity in the injection zone controls not only the accumulation and distribution of CO_2 within the reservoir, but also possible leakage pathways into the confining layers. High permeability pathways are apparent within the injection zone (Fig. 5D, E) where there are small amounts of CO_2 that are completely disconnected from the main portion of the plume. This is due to the spatial distribution of permeability and the pressure gradient caused by the injection. As CO_2 is injected and migrates out into the formation, the CO_2 reaches areas of low permeability, which can inhibit flow. This causes injection pressure to accumulate, which causes the CO_2 to take the path that is most energetically favorable. In some instances, this effect forces vertical CO_2 flow as shown in Fig. 5E. These results are congruent with those of Doughty and Pruess (2004) and show that there are high permeability pathways both horizontally and vertically. It is also important to note the control that the anisotropic permeability correlation structures exhibit on the accumulation and distribution of CO_2 in a single simulation. In simulation 20 (Fig. 5) the injected free-phase CO_2 has migrated ~2,400 m away from the injection in the direction of maximum spatial correlation (N40°E) (Fig. 5B), where as, CO_2 has only migrated ~1,100 m parallel to the direction of minimum spatial correlation (N130°E) (Fig. 5C).

The complete ensemble simulation results (e-type estimates) for free-phase supercritical CO_2 saturation after 20 years of injection are shown in Fig. 6. The ensemble mean CO_2 saturation in each injection layer, is a circular-shaped plume, which is similar to the individual model results from McGrail et al. (2009) and Bacon et al. (2014). Interestingly, these latter studies implement radially symmetric model domains with layered heterogeneity and internally homogeneous injection zones to simulate an injection of 1,000 MT of CO_2 at the Wallula Pilot Borehole. However, the large scale CO_2 injection simulated by McGrail et al. (2012) is more comparable to this study where they use a radially-symmetric grid to simulate an annual injection of 0.8 MMT supercritical CO_2 into the Grande Ronde formation and sub-basalt sediment layers and show that after 10 years of injection the CO_2 migrates ~500 m from the injection well and ~1,000 m after 30 years. In comparison to the results from McGrail et al. (2012), Fig. 6 illustrates after 20 years of a CO_2 injection that the plume migrates ~900 m from the injection well. Which suggests that the permeability correlation structure does not strongly influence the mean ensemble behavior of CO_2.

While the ensemble mean behavior of CO_2 from this study is similar to the results from studies with internally homogeneous injection reservoirs, the variability in this study reveals dramatically different

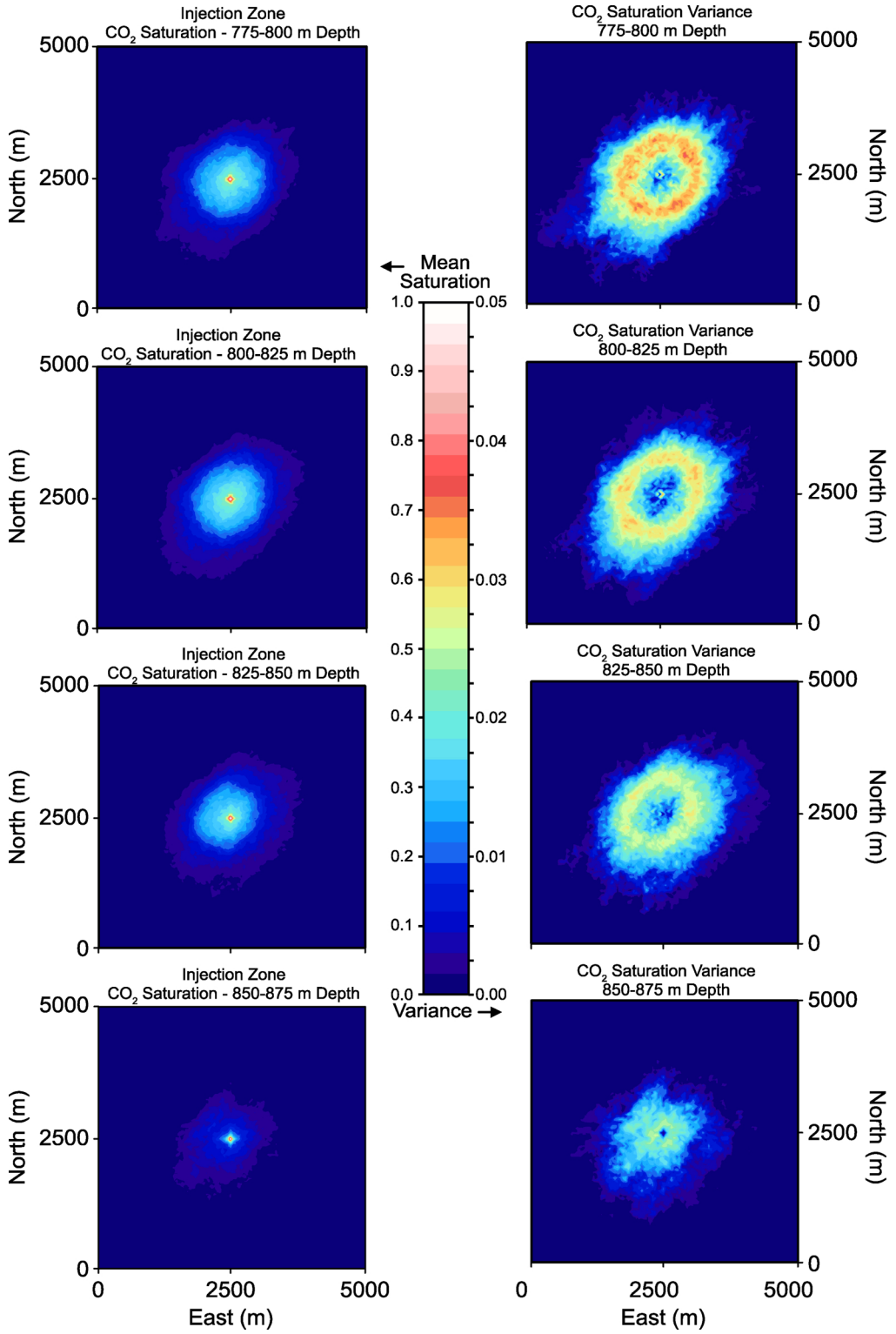

Fig. 6. E-type estimates for ($N = 50$) 20-year CO_2 injections. Average free-phase CO_2 saturation over all 50 simulations for the injection zones are shown on the left and the corresponding variance is shown on the right.

results. The variance of CO_2 saturation over all 50 simulations is shown in Fig. 6, which illustrates an 'ellipse' of variability extending up to ~1,800 m away from the injection well. The longitudinal axis of the ellipse trends N40°E, which is the direction of maximum spatial correlation. This result suggests that the uncertainty of CO_2 migration within CRBG basalt is strongly governed by the regional permeability correlation structure. This variability associated with the CO_2 plume is similar to the results of Pollyea and Fairley (2012), which implements a Monte Carlo simulation strategy to quantify the effects of spatial heterogeneity in low-volume basalt formations typical of the east Snake

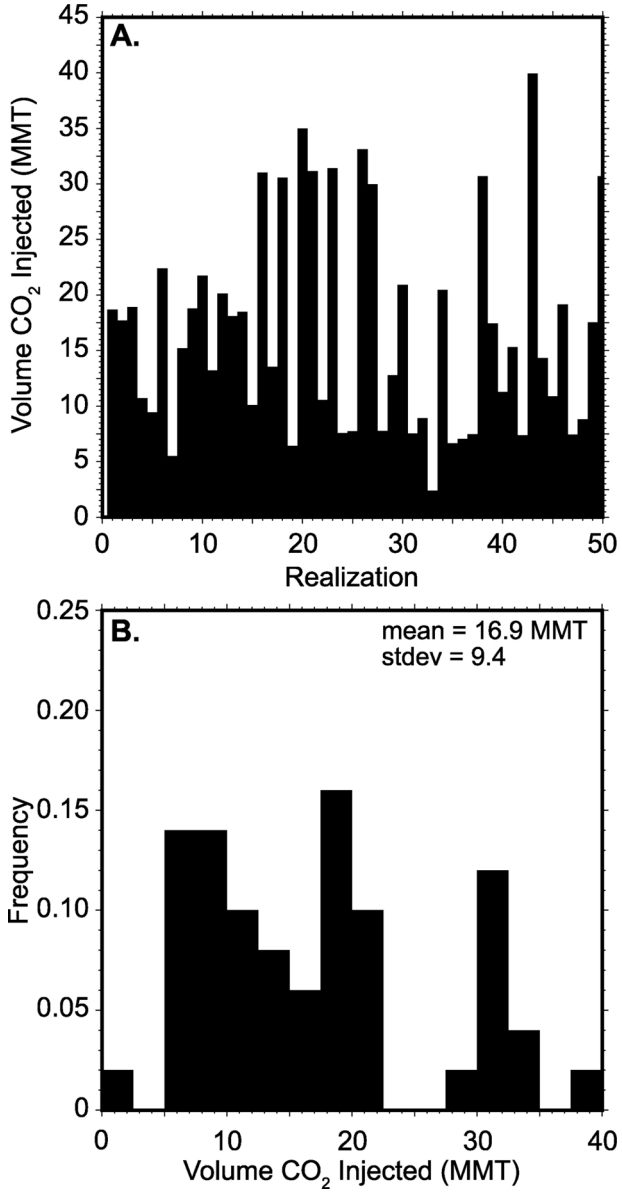

Fig. 7. A. Total volume of CO_2 (in million metric tons, MMT) injected after 20 years of simulation for each of the 50 realizations. B. Histogram of the total volume injected of all 50 simulations along with the mean and standard deviation of the volume injected.

River Plains, Idaho. In this study, the ensemble variance exhibits a similar 'ring of uncertainty' with a very large range of variability within the basalt reservoir. While these results are similar, these studies differ with respect to geologic media being studied (low-volume basalts versus flood basalts) and the correlation ranges use to create the permeability distributions. Pollyea and Fairley (2012) uses a geostatistical analysis of an outcrop scale low-volume basalt with a maximum correlation range of 38 m to simulate a reservoir-scale CO_2 injection, while this study uses a regional-scale geostatistical analysis with a correlation structure of 35 km presented by Jayne and Pollyea (2018). Overall, the ensemble analysis indicates that the mean CO_2 plume geometry exhibits a circular shape around the injector, while the variance corresponding with this result is strongly affected by the direction of maximum spatial permeability correlation.

The variability over all 50 simulations is not only obvious in the shape of the individual plumes (Fig. 5) and the ensemble variance (Fig. 6), but also in the total volume injected in each simulation. The total volume of CO_2 injected into each of the 50 equally probable synthetic reservoirs ranges from a nominal 2.4 MMT (0.12 MMT $year^{-1}$) to 40 MMT (2 MMT $year^{-1}$), as shown in Fig. 7. For reference, a small-scale 37 MW bio-mass fueled electric generator would emit ~0.8 MMT $year^{-1}$ (McGrail et al., 2012) and for a large-scale 1,000 MW gas-fired power plant would produce ~1.36 MMT $year^{-1}$ of CO_2. For equally-probable reservoirs, this is a significant amount of variability (Fig. 7B). If the scenario presented by McGrail et al. (2012) were implemented at the Wallula Borehole, the results from this study show that a constant pressure injection at 95% of the borehole breakout pressure would result in 60% of the equally probable reservoirs successfully accepting enough CO_2 to meet the criteria for a 37 MW electric generator. Conversely, that would mean that 40% of the synthetic reservoirs would fail with the given scenario and if a larger volume of injected CO_2 were required the chances of success would quickly decrease. For example, only 20% of the reservoirs would have the injectivity for a modest increase in the injection rate to 1.15 MMT $year^{-1}$. While the average injection rate varies between each simulation, a similar trend in injection rate over time within each simulation is observed. The injection rate over all 50 simulations is highest at the beginning of the simulation and over the course of the injection; the injection rate steadily decreases as the CO_2 displaces larger volumes of water. This decrease in injectivity over time is similar to the results of Burton et al. (2009), which shows the effects of the relative permeability curve on injection rate within a sandstone reservoir.

In order to visualize the variability in CO_2 injection volume for constant pressure injections, Fig. 8 illustrates the isosurface at 1% gas saturation for four individual realizations, which represent the simulation closest to the mean CO_2 volume (Fig. 8, realization 20), one standard deviation from the mean (Fig. 8 realization 11), and the minimum and maximum CO_2 volumes (Fig. 8, realizations 33 and 43, respectively). This variability in CO_2 plume shape and volume injected over the ensemble of simulations has important implications for MMV practices. There is a wide variety of methods available to monitor a CO_2 injection, such as, geophysical methods (e.g., seismic, electrical, gravity), pressure monitoring, well logging, fluid sampling, and soil gas monitoring. Each of these methods have their benefits but they also have drawbacks, e.g., detection occurs after potential impacts have occurred, significant effort for null result (Benson et al., 2006). Mathieson et al. (2010) discusses the monitoring and verification methods carried out at a CO_2 sequestration site in Algeria and emphasizes that CO_2 plume development is far from homogeneous and that each storage site is unique. This requires a specific monitoring program tailored to the risks at each site. The results presented here show that the average CO_2 plume behavior may exhibit characteristics of an isotropic permeability distribution, but the variability over all 50 simulations is significant, and warrants a site specific monitoring program. In the case of the Wallula Site, leakage from the composite injection zone into the bounding entablature layers is a concern due to the highly-fractured nature of the CBRG. E-type estimates for the layers bounding the composite injection zone are presented in Fig. 9. Owing to buoyancy forces, free-phase CO_2 migrates upward into the fractures within the flow interior and Fig. 5A, B illustrate how spatial heterogeneity in the injection layer impacts the CO_2 plume shape within the flow interior. While the CO_2 saturation in Fig. 9 is minimal compared to the injection zones, these results show that 0.1–1.05% of the total

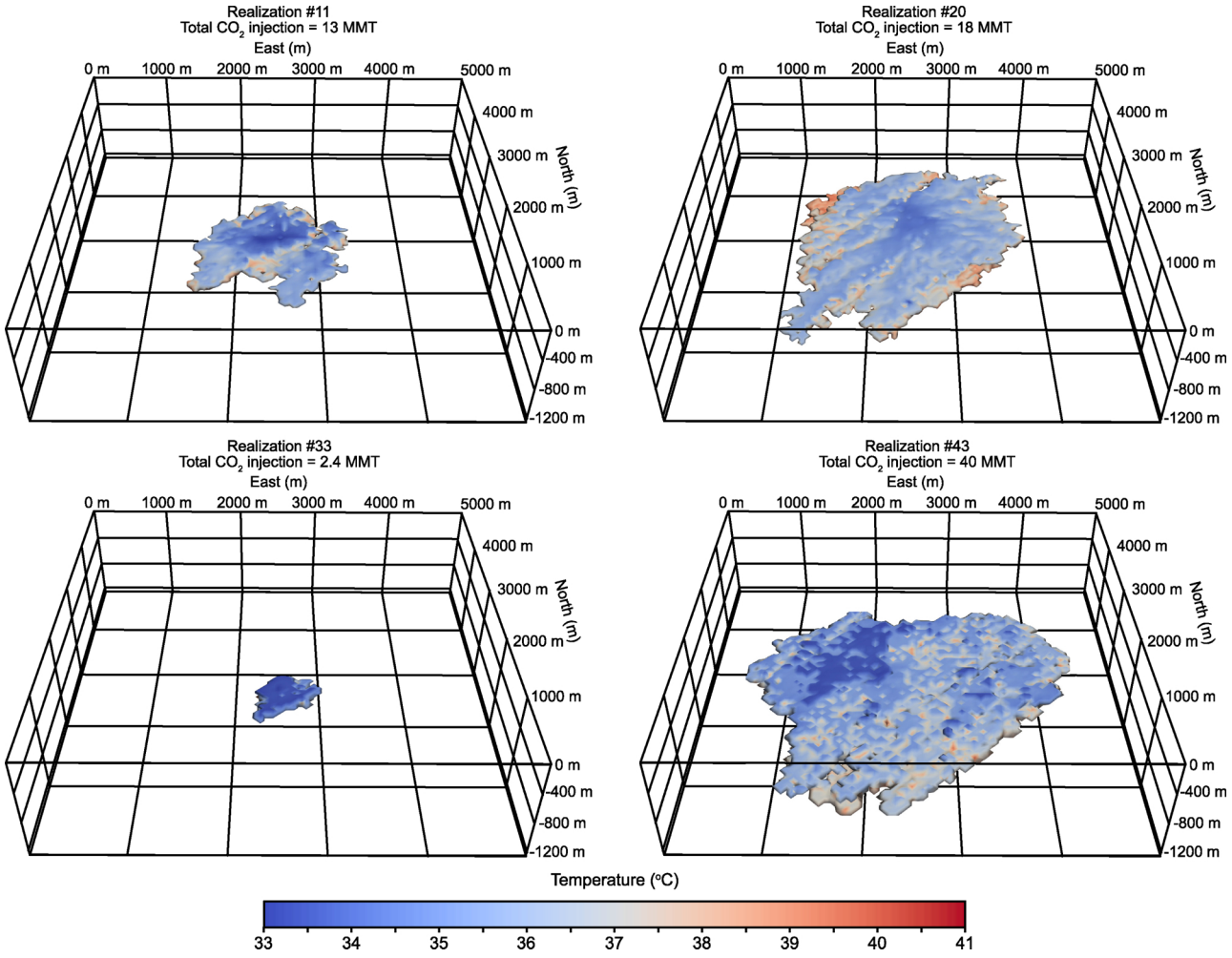

Fig. 8. Four different realizations that illustrate the variability in CO_2 plume shape and size after a 20-year CO_2 injection. Isosurface represents the edge of the CO_2 plume, each plume is contoured by temperature. Each realization is an equally-probable outcome for the given permeability dataset, note the different size, shape, and orientation of the CO_2 plumes.

volume injected has migrated outside of the composite injection zone. The USDOE (2013) requires that a successful CCS project keeps > 99% of the injected CO_2 isolated within the reservoir for one-thousand years. However, in no simulation did the injected CO_2 migrate farther than the layers immediately bounding the composite injection zone, which is an area for possible mineralization of the CO_2. These results are also congruent with the high-resolution fracture modeling of Gierzynski and Pollyea (2017), which shows that CO_2 flow tends to converge on a single flow path within a fracture network and suggests that this flow path convergence leads to a physical trapping mechanism followed by possible mineralization.

Additionally, results from this study indicate that the thermal effects of a CO_2 injection may also be used for MMV practices. Specifically, the change in reservoir temperature from pre- to post-injection shows that temperature within the reservoir changes ± 4 °C as a result of the CO_2 injection (Fig. 10). The areas that show the largest increase in temperature are near the edges of the plume, while areas that show the largest decrease in temperature are near the injection well. At the edges of the CO_2 plume, CO_2 dissolves into the reservoir water and releases heat, which is a process referred to as the heat of dissolution because CO_2 dissolution in water is an exothermic reaction (Pruess, 2005). In contrast, the cooling shown in this study is caused by Joule-Thomson expansion, which describes the temperature change associated with the expansion of a gas (Roebuck et al., 1942). During injections, the CO_2 is injected at a high pressure and begins to expand and cool as it migrates away from the injection well (Oldenburg, 2007). The competing effects of the heat of dissolution and Joule-Thomson expansion are shown in Figs. 8 and 10. The isosurfaces in Fig. 8 are contoured by temperature to illustrate the competing temperature effects of a large-scale CO_2 injection. As the CO_2 migrates away from the wellbore due to the pressure gradient imposed by the injection, the CO_2 begins to expand and cool, but at the edges of the plume the CO_2 is dissolving into the reservoir water and giving off enough heat to overcome Joule-Thomson cooling resulting in a net increase in temperature. Conversely, near the wellbore after some time the water becomes saturated and no more CO_2 will dissolve. At this point, Joule-Thomson cooling dominates resulting in a net decrease in temperature near the well (Fig. 10A–C and E). This result suggests that the competing effects of dissolution heating and Joule-Thomson cooling may be an effective strategy to monitor breakthrough. Namely, the heat of dissolution effect may be used to predict CO_2 breakthrough at monitoring wells within the reservoir. As the CO_2 dissolves into the reservoir water and releases heat, both the

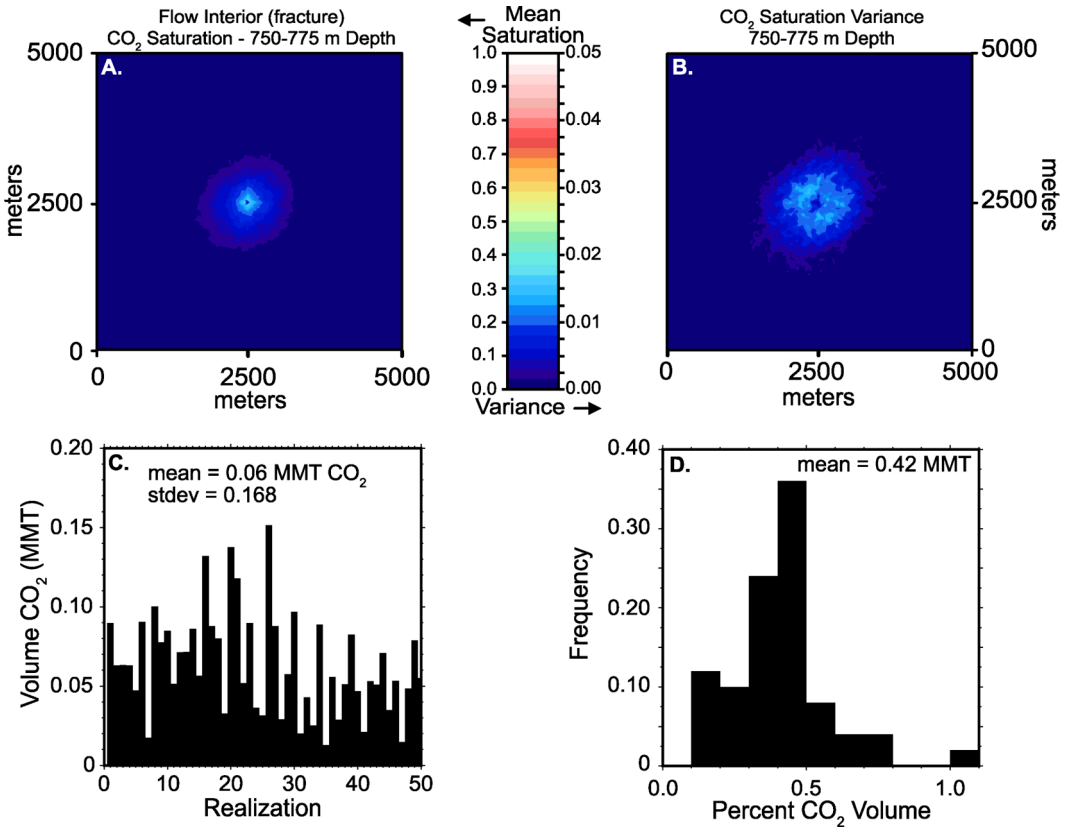

Fig. 9. A. E-type estimates for mean CO_2 saturation (A) and variance (B) for the flow interior layer bounding the injection zone. C. Total volume of CO_2 in million metric tons (MMT) within the flow interior. D. Histogram showing the percentage of the total volume injected that has migrated to into the flow interior.

CO_2 and reservoir water experience an increase in temperature. This results in a thermal anomaly that migrates throughout the reservoir slightly ahead of the free phase CO_2 plume. As a result, we would expect an increase in temperature would reach a monitoring well before the CO_2 plume. This effect is illustrated in Fig. 11, which shows how temperature and CO_2 saturation change over the course of the CO_2 injection at two monitoring locations 50 m away from the wellbore. In Fig. 11 the first change in temperature occurs after 6 days of simulation. Over the next 15 days the black line (red line shows a similar trend) steadily increases in temperature from 34.5 °C to 35.5 °C, then continues to increase in temperature up to 36.8 °C by day 26. At day 26, the maximum temperature at this monitoring location is reached, which occurs contemporaneously with the first appearance of CO_2. For the given simulation, two grid blocks located within the layer bounding the composite injection zone exhibit a steady increase in temperature until the arrival of CO_2 which suggests that temperature may be a proxy for CO_2 breakthrough because water drainage follows the same high permeability pathways as CO_2 imbibition. These results suggest that thermal monitoring may be an effective predictor of CO_2 breakthrough, however more research is needed in this area of study.

4. Conclusion

Flood basalts have been gaining recognition as potential reservoirs for carbon capture and sequestration. The success of recent field experiments in Washington State, USA, and Iceland have validated that injected CO_2 will interact with the basalt to form carbonate minerals at the field-scale and very short timescales. Upscaling these field-scale experiments is required if CCS is to be an effective strategy for mitigating the adverse effect of industrial CO_2 emissions. However, there are a number of uncertainties associated with upscaling to an industrial-scale CO_2 injection. For example, incomplete knowledge of multiphase flow in highly heterogeneous basalt reservoirs and detailed reservoir characterizations are required for proper numerical modeling and to effectively design a monitoring, measuring, and verification plan. This study investigates the uncertainty of a large-scale CO_2 injection into a highly heterogeneous basalt reservoir by focusing on the effects of spatially distributed permeability on CO_2 plume migration. For a sole CO_2 injection well operating within the CRBG at 95% of borehole breakout pressure, we find:

1. The aggregate behavior of the 50 simulations results in a concentric CO_2 plume shape around the injection well, which suggests that ensemble behavior is not governed by the spatial correlation structures.
2. Ensemble variance shows an ellipse of uncertainty around the CO_2 plume that extends up to 1,800 m away from the injection, this ellipse trends parallel to the direction of maximum spatial permeability correlation, suggesting that the uncertainty associated with a large-scale CO_2 injection is strongly controlled by the permeability correlation structures. This means that spatial variability must be accounted for to fully understand how variability propagates into operational and MMV decisions.
3. Injected CO_2 migrates from the injection zone into the entablature layer bounding the injection zone, but the CO_2 does not migrate any further suggesting that this region has the potential for CO_2-water-

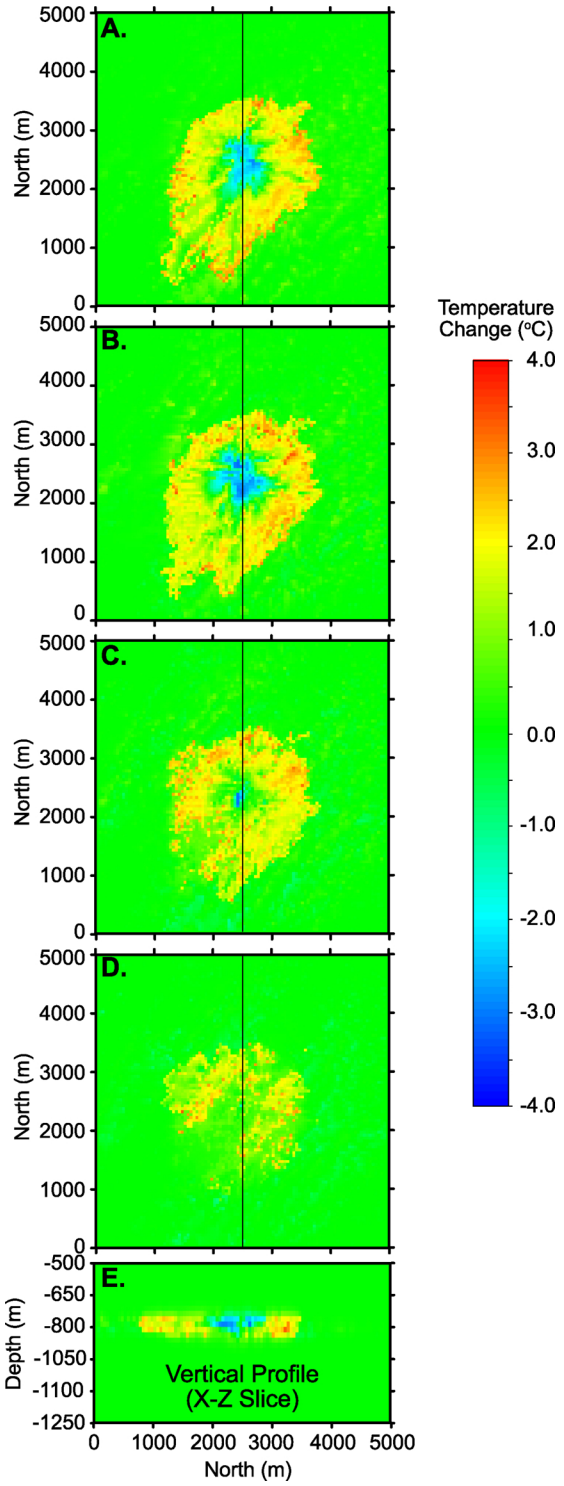

Fig. 10. Change in temperature between pre-CO_2 injection temperatures to post-CO_2 injection temperatures for a single realization (20). Panels A–D. Represent the 4 injection layers within the model domain. E. A vertical north-south profile through the center (indicated by the black lines in A-D) of the model domain.

basalt interactions to effectively isolate large-scale CO_2 injection volumes.

4. The volume of CO_2 injected at 95% of the borehole breakout pressure for 20 years ranges from 2.4 MMT (0.12 MMT $year^{-1}$) to 40.0 MMT (2.0 MMT $year^{-1}$). While the minimum volume injected only accommodates 15% of the volume required for the proposed scenario of offsetting the carbon emissions from a 37 MW generator. The maximum volume injected could support at 1,000 MW gas-fired power plant with a single injection.
5. Non-isothermal effects, namely the heat of dissolution associated with a large-scale CO_2 injection may be an effective MMV strategy for monitoring CO_2 breakthrough.

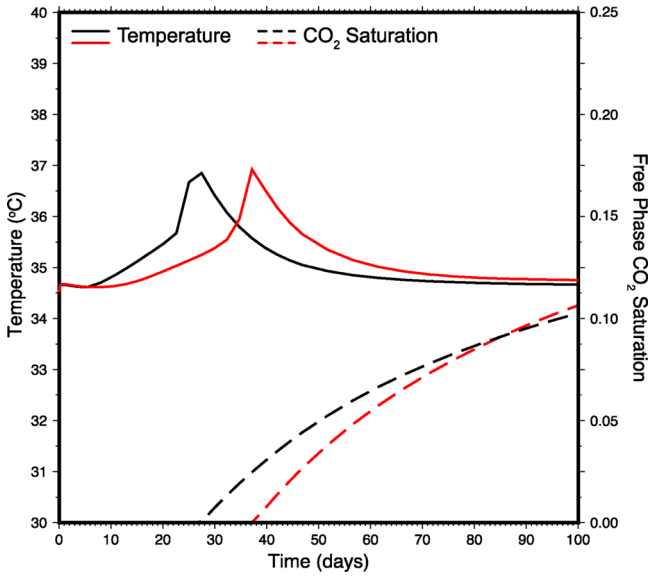

Fig. 11. Temperature and CO_2 saturation versus time for two monitoring locations within the confining layer (750–775 m depth) each 50 m away from the injection. The time lag between the black and red lines illustrates the effects of permeability heterogeneity. (For interpretation of the references to color in this figure legend, the reader is referred to the web version of this article.)

In conclusion, these results suggest that the implementation of a regional-data set and spatial correlation structures into a numerical model can provide insights into the behavior of CO_2 flow in highly heterogeneous reservoirs. Additionally, these results illustrate the uncertainty associated with highly-heterogeneous flood basalt reservoirs and a CCS project would require extensive reservoir characterization and a unique monitoring, measuring, and verification plan. Significantly more research is required to develop a better understanding of the reactive transport, geomechanical, and thermal processes associated with an industrial-scale CO_2 injection into a flood basalt reservoir.

Acknowledgments

We thank two anonymous reviewers for their thoughtful reviews of an early draft of this manuscript. We also thank editor Jean-Philippe Nicot for his careful stewardship of our manuscript. This study received financial support from the U.S. Department of Energy National Energy Technology Laboratory through cooperative agreement DE-FE0023381 (PI Pollyea).

References

Bachu, S., 2003. Screening and ranking of sedimentary basins for sequestration of CO_2 in geological media in response to climate change. Environ. Geol. 44, 277–289.

Bacon, D.H., Ramanathan, R., Schaef, H.T., McGrail, B.P., 2014. Simulating geologic co-sequestration of carbon dioxide and hydrogen sulfide in a basalt formation. Int. J. Greenh. Gas Control 21, 165–176.

Benson, S.M., et al., 2006. Monitoring carbon dioxide sequestration in deep geological formations for inventory verification and carbon credits. In: SPE Annual Technical Conference and Exhibition. Society of Petroleum Engineers.

Bosshart, N.W., Azzolina, N.A., Ayash, S.C., Peck, W.D., Gorecki, C.D., Ge, J., Jiang, T., Dotzenrod, N.W., 2018. Quantifying the effects of depositional environment on deep saline formation CO_2 storage efficiency and rate. Int. J. Greenh. Gas Control 69, 8–19.

Brennan, S.T., Burruss, R.C., 2003. Specific Sequestration Volumes: A Useful Tool for CO_2 Storage Capacity Assessment. US Department of the Interior, US Geological Survey.
Burns, E.R., Morgan, D.S., Peavler, R.S., Kahle, S.C., 2011. Three-Dimensional Model of the Geologic Framework for the Columbia Plateau Regional Aquifer System, Idaho, Oregon, and Washington. US Geological Survey Technical Report.
Burns, E.R., Williams, C.F., Tolan, T., Kaven, J.O., 2016. Are the Columbia River Basalts, Columbia Plateau, Idaho, Oregon, and Washington, USA, a Viable Geothermal Target? A preliminary analysis. Proceedings, 41st Workshop on Geothermal Reservoir Engineering.
Burton, M., Kumar, N., Bryant, S.L., 2009. CO_2 injectivity into brine aquifers: why relative permeability matters as much as absolute permeability. Energy Proc. 1, 3091–3098.
Chadwick, A., Arts, R., Bernstone, C., May, F., Thibeau, S., Zweigel, P., 2008. Best Practice for the Storage of CO_2 in Saline Aquifers-Observations and Guidelines from the SACS and CO_2STORE Projects, vol. 14 British Geological Survey.
Chang, C., Zhou, Q., Kneafsey, T.J., Oostrom, M., Wietsma, T.W., Yu, Q., 2016. Pore-scale supercritical CO_2 dissolution and mass transfer under imbibition conditions. Adv. Water Resour. 92, 142–158.
Deutsch, C.V., Journel, A.G., 1998. GSLIB: Geostatistical Software Library and User's Guide. Oxford University Press, New York.
Doughty, C., 2010. Investigation of CO_2 plume behavior for a large-scale pilot test of geologic carbon storage in a saline formation. Transp. Porous Media 82, 49–76.
Doughty, C., Pruess, K., 2004. Modeling supercritical carbon dioxide injection in heterogeneous porous media. Vadose Zone J. 3, 837–847.
Gephart, R., Price, S., Jackson, R., Myers, C., 1983. Geohydrologic factors and current concepts relevant to characterization of a potential nuclear waste repository site in Columbia River Basalt, Hanford Stte, Washington. In: MRS Proceedings. Cambridge Univ Press. pp. 85.
Gierzynski, A.O., Pollyea, R.M., 2017. Three-phase CO_2 flow in a basalt fracture network. Water Resour. Res. 53, 8980–8998.
Jayne, R.S., Pollyea, R.M., 2018. Permeability correlation structure of the columbia river plateau and implications for fluid system architecture in continental large igneous provinces. Geology 46, 715–718.
Jung, Y., Pau, G.S.H., Finsterle, S., Pollyea, R.M., 2017. TOUGH3: a new efficient version of the TOUGH suite of multiphase flow and transport simulators. Comput. Geosci. 108, 2–7.
Kahle, S., Morgan, D., Welch, W., Ely, D., Hinkle, S., Vaccaro, J., Orzol, L., 2011. Hydrogeologic Framework and Hydrologic Budget Components of the Columbia Plateau Regional Aquifer System, Washington, Oregon, and Idaho. US Geological Survey Technical Report.
Li, Y., LeBoeuf, E.J., Basu, P.K., Mahadevan, S., 2005. Stochastic modeling of the permeability of randomly generated porous media. Adv. Water Resour. 28, 835–844.
Litynski, J.T., Klara, S.M., McIlvried, H.G., Srivastava, R.D., 2006. The United States Department of Energy's regional carbon sequestration partnerships program: a collaborative approach to carbon management. Environ. Int. 32, 128–144.
Mangan, M.T., Wright, T.L., Swanson, D.A., Byerly, G.R., 1986. Regional correlation of Grande Ronde Basalt flows, Columbia River Basalt Group, Washington, Oregon, and Idaho. Geol. Soc. Am. Bull. 97, 1300–1318.
Mathieson, A., Midgley, J., Dodds, K., Wright, I., Ringrose, P., Saoul, N., 2010. CO_2 sequestration monitoring and verification technologies applied at Krechba, Algeria. Lead. Edge 29, 216–222.
Matter, J.M., Kelemen, P.B., 2009. Permanent storage of carbon dioxide in geological reservoirs by mineral carbonation. Nat. Geosci. 2, 837–841.
Matter, J.M., Stute, M., Snæbjörnsdottir, S.Ó., Oelkers, E.H., Gislason, S.R., Aradottir, E.S., Sigfusson, B., Gunnarsson, I., Sigurdardottir, H., Gunnlaugsson, E., et al., 2016. Rapid carbon mineralization for permanent disposal of anthropogenic carbon dioxide emissions. Science 352, 1312–1314.
Matter, J.M., Takahashi, T., Goldberg, D., 2007. Experimental evaluation of in situ CO_2-water–rock reactions during CO_2 injection in basaltic rocks: implications for geological CO_2 sequestration. Geochem. Geophys. Geosyst. 8.
McGrail, B., Freeman, C., Brown, C., Sullivan, E., White, S., Reddy, S., Garber, R., Tobin, D., Gilmartin, J., Steffensen, E., 2012. Overcoming business model uncertainty in a carbon dioxide capture and sequestration project: case study at the Boise White Paper Mill. Int. J. Greenh. Gas Control 9, 91–102.
McGrail, B., Spane, F., Sullivan, E., Bacon, D., Hund, G., 2011. The Wallula basalt sequestration pilot project. Energy Proc. 4, 5653–5660.
McGrail, B., Sullivan, E., Spane, F., Bacon, D., Hund, G., Thorne, P., Thompson, C., Reidel, S., Colwell, F., 2009. Topical Report-Preliminary Hydrogeologic Characterization Results from the Wallula Basalt Pilot Study. Pacific Northwest National Laboratory Technical Report. Report PNWD-4129.
McGrail, B.P., Schaef, H.T., Ho, A.M., Chien, Y.J., Dooley, J.J., Davidson, C.L., 2006. Potential for carbon dioxide sequestration in flood basalts. J. Geophys. Res.: Solid Earth 111.
McGrail, B.P., Schaef, H.T., Spane, F.A., Cliff, J.B., Qafoku, O., Horner, J.A., Thompson, C.J., Owen, A.T., Sullivan, C.E., 2017. Field validation of supercritical CO_2 reactivity with basalts. Environ. Sci. Technol. Lett. 4, 6–10.
Van der Meer, L., 1995. The CO_2 storage efficiency of aquifers. Energy Convers. Manag. 36, 513–518.
Metz, B., Davidson, O., De Coninck, H., Loos, M., Meyer, L., 2005. IPCC Special Report on Carbon Dioxide Capture and Storage. Technical Report. Intergovernmental Panel on Climate Change, Geneva (Switzerland) Working Group III.
Navarre-Sitchler, A.K., Maxwell, R.M., Siirila, E.R., Hammond, G.E., Lichtner, P.C., 2013. Elucidating geochemical response of shallow heterogeneous aquifers to CO_2 leakage using high-performance computing: implications for monitoring of CO_2 sequestration. Adv. Water Resour. 53, 45–55.
NETL, 2011. Best Practices for: Risk Analysis and Simulation of Geologic Storage of CO_2. DOE/NETL-2011/1459.
Neufeld, J.A., Vella, D., Huppert, H.E., 2009. The effect of a fissure on storage in a porous medium. J. Fluid Mech. 639, 239–259.
Oldenburg, C., Lewicki, J., 2006. On leakage and seepage of CO_2 from geologic storage sites into surface water. Environ. Geol. 50, 691–705.
Oldenburg, C.M., 2007. Joule-Thomson cooling due to CO_2 injection into natural gas reservoirs. Energy Convers. Manag. 48, 1808–1815.
Pawar, R.J., Watson, T.L., Gable, C.W., 2009. Numerical simulation of CO_2 leakage through abandoned wells: model for an abandoned site with observed gas migration in Alberta, Canada. Energy Proc. 1, 3625–3632.
Pollack, H.N., Hurter, S.J., Johnson, J.R., 1993. Heat flow from the Earth's interior: analysis of the global data set. Rev. Geophys. 31, 267–280.
Pollyea, R.M., 2016. Influence of relative permeability on injection pressure and plume configuration during CO_2 injections in a mafic reservoir. Int. J. Greenh. Gas Control 46, 7–17.
Pollyea, R.M., Fairley, J.P., 2012. Implications of spatial reservoir uncertainty for CO_2 sequestration in the east Snake River Plain, Idaho (USA). Hydrogeol. J. 20, 689–699.
Pollyea, R.M., Fairley, J.P., Podgorney, R.K., Mcling, T.L., 2014. Physical constraints on geologic CO_2 sequestration in low-volume basalt formations. Geol. Soc. Am. Bull. 126, 344–351.
Pollyea, R.M., Rimstidt, J.D., 2017. Rate equations for modeling carbon dioxide sequestration in basalt. Appl. Geochem. 81, 53–62.
Popova, O.H., Small, M.J., McCoy, S.T., Thomas, A., Rose, S., Karimi, B., Carter, K., Goodman, A., 2014. Spatial stochastic modeling of sedimentary formations to assess CO_2 storage potential. Environ. Sci. Technol. 48, 6247–6255.
Price, P.N., Oldenburg, C.M., 2009. The consequences of failure should be considered in siting geologic carbon sequestration projects. Int. J. Greenh. Gas Control 3, 658–663.
Pruess, K., 1992. Brief Guide to the MINC-Method for Modeling Flow and Transport in Fractured Media. Earth Science Division. Lawrence Berkeley Laboratory, University of California, Berkeley, pp. 10179.
Pruess, K., 2005. Numerical simulations show potential for strong nonisothermal effects during fluid leakage from a geologic disposal reservoir for CO_2. Dyn. Fluids Transp. Fract. Rock 81–89.
Pruess, K., 2011. ECO_2M: a TOUGH2 fluid property module for mixtures of water, NaCl, and CO_2, including super-and sub-critical conditions, and phase change between liquid and gaseous CO_2. Ernest Orlando Lawrence Berkeley National Laboratory, Berkeley, CA (US) Technical Report.
Pruess, K., Garcia, J., 2002. Multiphase flow dynamics during CO_2 disposal into saline aquifers. Environ. Geol. 42, 282–295.
Pruess, K., Xu, T., Apps, J., Garcia, J., 2003. Numerical Modeling of Aquifer Disposal of CO_2. SPEJ 8 (1): 49–60. Technical Report. SPE-83695-PA. https://doi.org/10.2118/83695-PA.
Reidel, S.P., Spane, F.A., Johnson, V.G., 2002. Natural Gas Storage in Basalt Aquifers of the Columbia Basin, Pacific Northwest USA: A Guide to Site Characterization. Pacific Northwest National Laboratory (PNNL), Richland, WA (US) Technical Report.
Rodosta, T., Litynski, J., Plasynski, S., Spangler, L., Finley, R., Steadman, E., Ball, D., Hill, G., McPherson, B., Burton, E., et al., 2011. US Department of Energy's regional carbon sequestration partnership initiative: update on validation and development phases. Energy Proc. 4, 3457–3464.
Roebuck, J., Murrell, T., Miller, E., 1942. The Joule-Thomson effect in carbon dioxide. J. Am. Chem. Soc. 64, 400–411.
Srivastava, R.M., 1994a. An overview of stochastic methods for reservoir characterization. AAPG Comput. Appl. Geol. 3–16.
USDOE, 2013. Carbon Technology Program Plan. Technical Report.
Wu, H., Jayne, R.S., Pollyea, R.M., 2018. A parametric analysis of capillary pressure effects during geologic carbon sequestration in a sandstone reservoir. Greenh. Gases Sci. Technol. 8 (6), 1039–1052.
Zakharova, N.V., Goldberg, D.S., Sullivan, E.C., Herron, M.M., Grau, J.A., 2012. Petrophysical and geochemical properties of Columbia River flood basalt: Implications for carbon sequestration. Geochem. Geophys. Geosyst. 13.